Applied Meteorology Unit (AMU)
Quarterly Report
Fourth Quarter FY-97

Contract NAS10-96018

31 October 1997

Distribution:

NASA HQ/M-7/S. Oswald
NASA HQ/Q/F. Gregory
NASA HQ/M/W. Trafton
NASA HQ/AS/F. Cordova
NASA KSC/PH/R. Sieck
NASA KSC/PH/J. Harrington
NASA KSC/AA-C/L. Shriver
NASA KSC/AA/R. Bridges
NASA KSC/MK/D. McMonagle
NASA KSC/PH-B/M. Wetmore
NASA KSC/PH-B3/J. Zysko
NASA KSC/PH-B3/J. Madura
NASA KSC/PH-B3/F. Merceret
NASA KSC/DE-TPO/K. Riley
NASA KSC/FF-R-B/P. McCalman
NASA JSC/MA/T. Holloway
NASA JSC/ZS8/F. Brody
NASA JSC/MS-4/W. Ordway
NASA JSC/DA8/J. Bantle
NASA MSFC/EL23/D. Johnson
NASA MSFC/SA0-1/A. McCool
NASA MSFC/EL23/S. Pearson
45 WS/DOR/W. Tasso
45 WS/SY/D. Harms
45 WS/SYA/B. Boyd
45 RANS/CC/S. Liburdi
45 OG/CC/P. Benjamin
45 MXS/CC/J. Hanigan
45 LG/LGQ/R. Fore
CSR 1300/M. Maier
CSR 4140/H. Herring
45 SW/SESL/D. Berlinrut
SMC/CWP/D. Carroll
SMC/CWP/J. Rodgers
SMC/CWP/T. Knox
SMC/CWP/R. Bailey
SMC/CWP (PRC)/P. Conant
Hq AFSPC/DDOR/G. Wittman
Hq AFMC/DOW/P. Yavosky
Hq AFWA/CC/J. Hayes
Hq AFWA/DNXT/D. Meyer
Hq AFWA/DN/L. Freeman
Hq USAF/XOW/F. Lewis
AFCCC/CCN/M. Adams
Office of the Federal Coordinator for Meteorological Services and Supporting Research
SMC/SDEW/B. Hickel
SMC/MEEV/G. Sandall
NOAA "W/OM"/L. Uccellini
NOAA/OAR/SSMC-I/J. Golden
NOAA/ARL/J. McQueen

NWS Melbourne/B. Hagemeyer
NWS/SRHQ/H. Hassel
NWS "W/SR3"/D. Smith
NSSL/D. Forsyth
NWS/"W/OSD5"/B. Saffle
NWS/"W/OSD23"/D. Kitzmiller
PSU Department of Meteorology/G. Forbes
FSU Department of Meteorology/P. Ray
NCAR/J. Wilson
NCAR/Y. H. Kuo
30 WS/CC/C. Davenport
30 WS/DOS/S. Sambol
30 WS/DO/C. Crosiar
30 SW/XP/R. Miller
NOAA/ERL/FSL/J. McGinley
Halliburton/NUS Corp./H. Firstenberg
ENSCO ARS Div. V.P./J. Pitkethly
ENSCO Contracts/M. Penn

Executive Summary

This report summarizes AMU activities for the fourth quarter of FY 97 (July-September). A detailed AMU project schedule is included in the Appendix.

During this quarter, AMU personnel supported two expendable vehicle launches and one Shuttle mission at Range Weather Operations. Dr. Manobianco traveled to JSC to observe SMG operations during the landing of STS-94 on 17 July. The purpose of the visit was to gain additional insight into the duties of SMG forecasters during Shuttle landing operations. He presented results from the AMU's meso-eta model evaluation to SMG staff and an overview of the AMU to selected SMG staff, Mr. Wayne Hale (ascent/entry flight director), Mr. Ed Gonzalez (flight dynamics office), Mr. Dan Menzel and Mr. Dan Grise (descent analysis/WINDS).

At the beginning of the quarter, Dr. Taylor and Ms. Lambert informed NWS MLB, SMG, and the 45 WS that the thunderstorm forecasting objective of the 915 MHz profiler task could not be completed due to operational problems with several of the profilers in the network. However, enough data had been collected to execute the data quality control (QC) objective as planned. Color displays of wind speed and direction have been developed for the raw and QC'd data. These displays highlight the areas of bad data and facilitate analysis of the effectiveness of the QC routines used. Large and small median filters have been implemented which check for temporal and spatial consistency in the data. Their results are shown in this report.

Mr. Evans is analyzing the plume resulting from the Delta II explosion on 17 January 1997 using WSR-88D radar observations and the atmospheric models REEDM, RAMS, and HYPACT. Radar reflectivity images provide good estimates of the location and dimensions of the plume. Model output from HYPACT is in relatively good agreement with the observations with the exception that the modeled plume moved onshore approximately 15 km south of the observed location.

Mr. Evans began work on the Model Validation Program Data Analysis project in July. The primary purpose is to produce RAMS and HYPACT data for the three MVP sessions conducted at Cape Canaveral in 1995-96. The source term configurations were determined and simulations were done for all of the continuous plume releases for Session III.

Dr. Taylor, Dr. Manobianco, and Mr. Nutter finished writing the task plan for the extension of the objective portion of the meso-eta model evaluation. This component of the evaluation is extended to include the warm and cool season periods from May through August 1997 and October 1997 through January 1998, respectively. A comparison between results from the 1996 and 1997 seasons will highlight changes in the error characteristics which may have occurred in response to updates in the meso-eta model configuration. Results from the 2-m temperature and 10-m wind analyses are presented in this report.

Dr. Taylor, Dr. Manobianco, and Mr. Nutter developed the formal task plan for the data assimilation model/central Florida data deficiency task. The three components of the task are to identify all meteorological data sources within 160 km of KSC/CCAS, identify an appropriate data assimilation model that can incorporate those data sources, and implement a working prototype of the identified model. The goal for running a local data integration system is to generate products which may enhance weather nowcasts and short-range (< 6 h) forecasts issued in support of 45 WS, SMG, and NWS MLB operational weather requirements.

In this quarter, Dr. Merceret briefed Chris Lessman (JSC), Steve Pearson (MSFC) and Richard Leach (MSFC) on the mid-tropospheric wind change climatology and it's consequences for risk analysis. He completed the range section of Tim Wilfong's profiler review paper for the *Bulletin of the American Meteorological Society*. His revised paper "Risk Assessment Consequences of the Lognormal Distribution of Midtropospheric Wind Changes" was accepted by the *Journal of Spacecraft and Rockets*.

SPECIAL NOTICE TO READERS

AMU Quarterly Reports are now published on the Wide World Web (WWW). The Universal Resource Locator for the AMU Home Page is:

http://technology.ksc.nasa.gov/WWWaccess/AMU/home.html

The AMU Home Page can also be accessed via links from the NASA KSC Internal Home Page alphabetical index. The AMU link is "CCAS Applied Meteorology Unit".

If anyone on the current distribution would like to be removed and instead rely on the WWW for information regarding the AMU's progress and accomplishments, please respond to Frank Merceret (407-853-8200, francis.merceret-1@ksc.nasa.gov) or Ann Yersavich (407-853-8203, anny@fl.ensco.com).

1. BACKGROUND

The AMU has been in operation since September 1991. The progress being made in each task is discussed in Section 2 with the primary AMU point of contact reflected on each task and/or subtask.

2. AMU ACCOMPLISHMENTS DURING THE PAST QUARTER

2.1 TASK 001 AMU OPERATIONS

During July, AMU personnel supported two expendable launches and one Shuttle mission at Range Weather Operations (RWO). In addition, Dr. Manobianco traveled to JSC to observe SMG operations prior to and during the landing of STS-94 on 17 July. The purpose of Dr. Manobianco's visit was to gain additional insight into the duties and responsibilities of SMG forecasters during Shuttle landing operations. He attended the MMT L-1 briefing and observed SMG operations and forecast briefings during the period L-2 through landing. Dr. Manobianco presented results from the AMU's meso-eta model evaluation to SMG staff and also an overview of the AMU to selected SMG staff, Mr. Wayne Hale (ascent/entry flight director), Mr. Ed Gonzalez (flight dynamics office), Mr. Dan Menzel and Mr. Dan Grise (descent analysis/WINDS).

SUBTASK 3 MICROBURST DAY POTENTIAL INDEX (MDPI) EVALUATION (MR. WHEELER)

Mr. Wheeler collected and analyzed data needed for the summer 1997 evaluation of the MDPI. The data will be merged with the 1995 data used in the previous MDPI final report (June 1996) and new statistics and threshold values will be computed. A final memorandum will be distributed upon completion on the analysis in early October.

2.2 TASK 004 INSTRUMENTATION AND MEASUREMENT

SUBTASK 1 NEXRAD EXPLOITATION (MR. WHEELER)

Mr. Wheeler finished his analysis of the four case days (11 July 1995, 13 August 1996, 29 March 1997, and 23 April 1997) for the Cell Trends Task using WATADS Build 9 during the past quarter. The cell trend attribute data (maximum reflectivity, height of the maximum reflectivity, storm top, storm base, hail and severe hail probabilities, SCIT VIL and core aspect ratio) are being entered into a spreadsheet. Once completed, trends and thresholds will be analyzed for using each cell's attributes. Work also began on developing an outline for the final report.

SUBTASK 2 915 MHZ BOUNDARY LAYER PROFILERS (DR. TAYLOR)

In June, Dr. Taylor and Ms. Lambert informed NWS MLB, SMG, and the 45 WS that at least four of the profilers must operate 90% of the time daily between 1400 and 0000 UTC from 1 July through 1 September 1997 to effectively evaluate the profiler network for its use in thunderstorm forecasting. This requirement had not been met by 1 July nor at any time during the month of July. Thus, the thunderstorm forecasting objective was deleted from the task in mid-July.

The data quality objective, however, was not affected and is being executed as planned. Algorithms have been developed to quality control (QC) the data, and color displays of wind speed and direction have been developed for the raw and QC'd data. These color displays highlight the areas of bad data and facilitate analysis of the effectiveness of the QC routines used.

A description of the profiler network, the current algorithms, and preliminary results of the QC are given below. Other QC algorithms will be developed and discussed in future reports.

The 915 MHz Profiler Network

The USAF 45 WS installed a network of five 915 MHz Doppler Radar Wind Profilers (DRWP) with Radio Acoustic Sounding Systems (RASS) in the KSC/CCAS area (Heckman et al. 1996). The profilers are arranged in a diamond-like pattern over the Cape area with an average spacing of 10-15 km, as seen in Figure 1. This network can provide three-dimensional wind direction and speed estimates in the boundary layer from 120 m to 4 km AGL and virtual temperature (T_v) estimates from 120 m to 1.5 km AGL. These profilers were installed to provide high spatial and temporal resolution wind profile data in the data gap between the top of the KSC/CCAS wind tower network (150 m) and the lowest gate (2 km) of the NASA 50 MHz DRWP.

The profilers are capable of operating in a five-beam configuration: one vertical beam and four oblique beams at a 23.5° angle from the zenith. They all currently use a three-beam configuration with one vertical and two oblique beams. The three-beam configuration was chosen to produce the highest possible temporal resolution consensus data without sacrificing accuracy in the three-dimensional wind calculations. The beam directions at each individual site were chosen to minimize potential interference from ground clutter (trees, aircraft, traffic, etc.).

The operational performance parameters of the profilers in the network are shown in Table 1.

The QC Algorithms

Two QC algorithms are applied to the data. The first is a large median filter which flags large areas of erroneous data. This is followed by a small median filter which flags individual data points. These median filters check the temporal and spatial consistency of the data. The equations used in the algorithms are adaptations of the routines developed in Carr et al (1995).

Large Median Filter

In this algorithm, a 6X6 box of wind data points in space and time is defined. Based on the data time and space resolution, this represents a time period of 1.5 hours and a height range of approximately 600 m. The median value for the u- and v-components of all good data points in the box is calculated. At least 19 of the 36 points must have unflagged consensed data.

The observations in the 5X5 interior box are checked against a critical threshold value, T, which is a function of the median of the u- and v-components and the altitude. The observation is flagged as bad if the absolute value of the difference between the observed and median components is greater than T.

This procedure is repeated for all possible 6X6 boxes in a 24-h period.
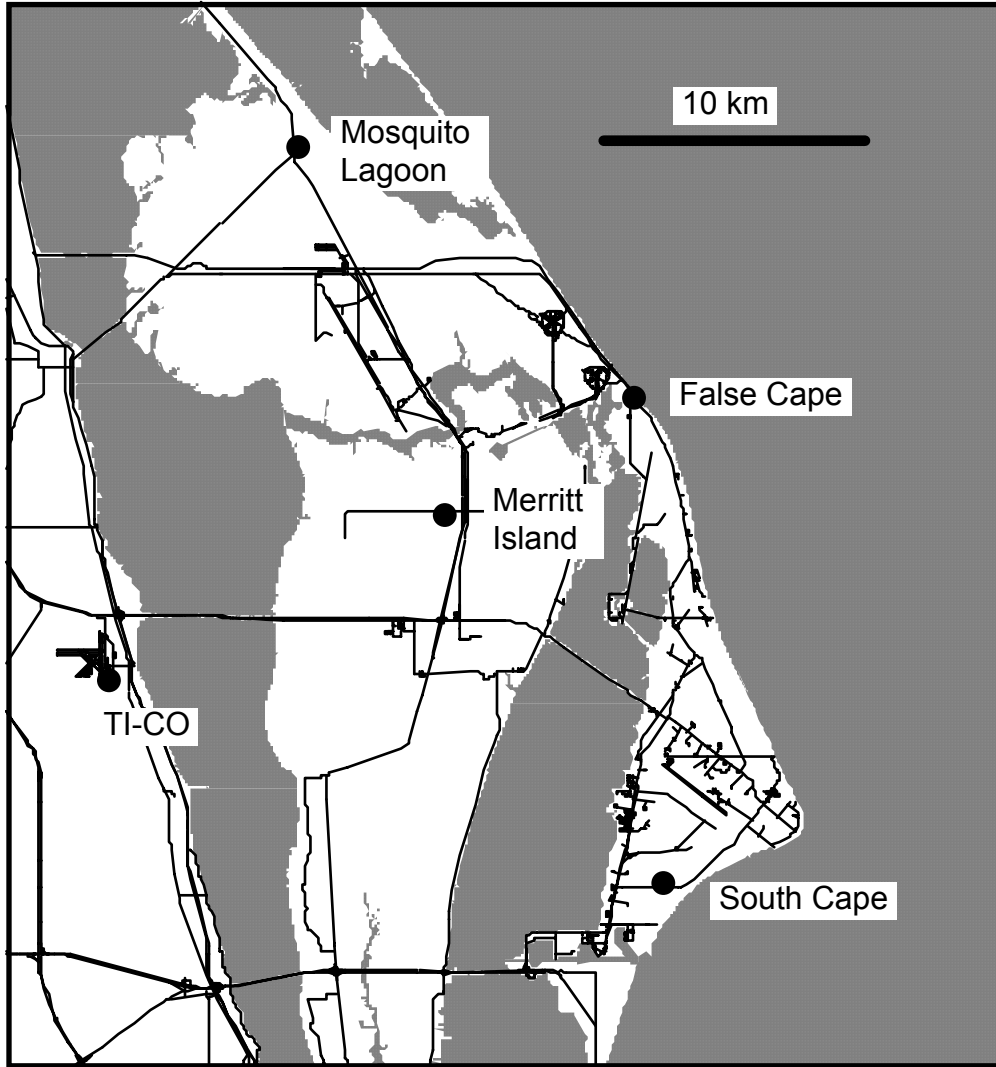
Figure 1.   The 915 MHz DRWP locations are indicated by a solid circle. The names of the locations are printed next to the circles, and a scale is provided in the upper-right.

Table 1. 915 MHz DRWP operational performance parameters.		
Parameter	*Wind*	*RASS (T_v)*
First gate height	117 m	112 m
Maximum height	3.1 km	1.4 km
Gate spacing	97 m	97 m
Number of gates	32	14
Nyquist velocity	10.1 ms^{-1}	412.5 ms^{-1}
Accuracy	Speed: < 1 ms^{-1} Direction: < 10°	1° C
Consensus period *	10 min	5 min
* The 10-minute consensus wind period is followed by the 5-minute T_v consensus period. Thus, consensus data are provided every 15 minutes		

Small Median Filter

The small median filter algorithm defines a 3X3 space and time box representing 45 minutes and 300 m. As with the large median filter, the median value for the u- and v-components of all good data points in the box is calculated. At least 5 of the 9 points must have unflagged consensed data.

The single observation in the center of the box is checked against a critical threshold value, T, as in the large median filter. This procedure is repeated for all possible 3X3 boxes in a 24-h period.

Preliminary Results

The results of the data QC using the large and small median filters are shown using data from the False Cape profiler (see Figure 1) collected on 17 June 1997. Color displays of wind speed and direction are used to help locate the obvious areas of erroneous data.

On 17 June, thunder showers were reported over the KSC/CCAS area beginning at 1630 UTC and extending to 2200 UTC, the same period over which most of the erroneous profiles were seen.

Figures 2 and 3 show the wind speed and direction, respectively, before the data QC. The black areas show the levels at which a consensus was not reached. The bad data can be identified by inconsistencies in time and space of both the wind speed and direction. Most notable are the inconsistencies found between 1700 - 1800 UTC from approximately 5000' - 10000', between 1930 - 2000 UTC through the entire profile, between 2030 - 2100 UTC from 7000' - 10000', and at 2130 from 3000' - 7000'.

Figures 4 and 5 show the wind speed and direction, respectively, after the data QC. The black areas show the levels where data were flagged as bad in addition to those levels where a consensus was not reached. Most of the bad data have been removed, but some bad data still remain at 1800 UTC from 5000' - 6000' and at 2000 UTC from 5500' - 7000'.

Summary

The results show that the large and small median filters are effective in flagging most of the erroneous consensus data. Further testing of different values in the median filter equations will be conducted which may yield better results.

The results also demonstrate the importance of using color displays of the data to find inconsistencies in the profiles that would indicate bad data. This information is used to look at the data values in the bad profiles to help determine threshold and constant values in the QC algorithms.
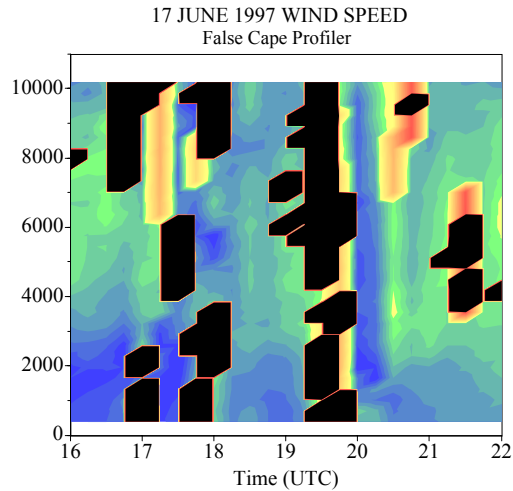
Figure 2. 17 June 1997 False Cape profiler display of wind speed from 1600 to 2200 UTC before data QC. Heights are in feet and wind speeds are in knots.
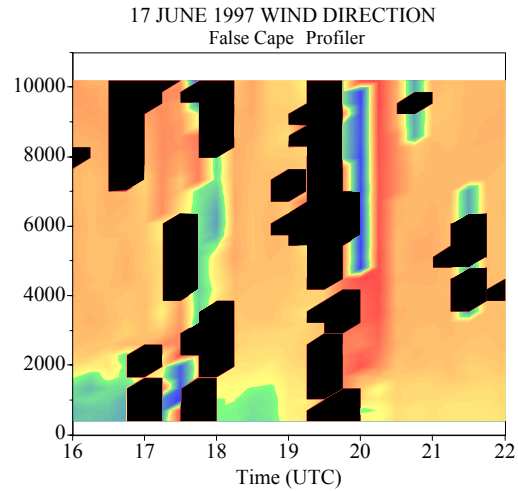
Figure 3. 17 June 1997 False Cape profiler display of wind direction from 1600 to 2200 UTC before data QC. Heights are in feet and wind directions are in degrees.
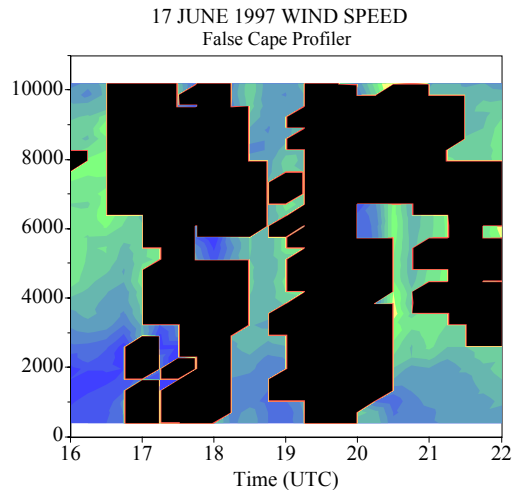
Figure 4. 17 June 1997 False Cape profiler display of wind speed from 1600 to 2200 UTC after the data QC. Heights are in feet and wind speeds are in knots.
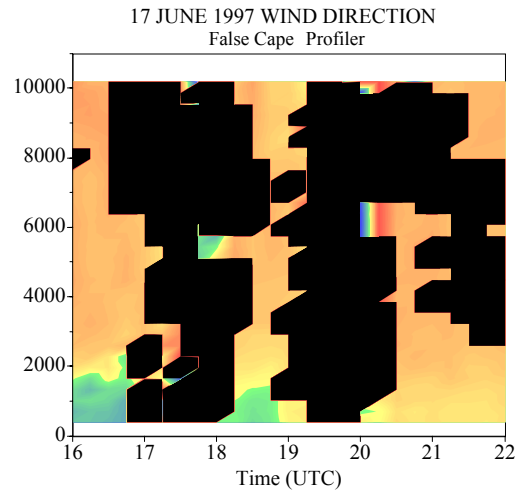
Figure 5. 17 June 1997 False Cape profiler display of wind direction from 1600 to 2200 UTC after data QC. Heights are in feet and wind directions are in degrees.

References

Carr, F. H., P. L. Spencer, C. A. Doswell III, and J. D. Powell, 1995: A comparison of two objective analysis techniques for profiler time-height data. *Mon. Wea. Rev.*, **123**, 2165 - 2180.

Heckman, S. T., M. W. Maier, W. P. Roeder, J. B. Lorens, and B. F. Boyd, 1996: The operational use of a boundary layer profiler network at the Eastern Range and Kennedy Space Center, *27th Conference on Radar Meteorology*, Vail, CO, 346-348.

SUBTASK 4   WARNING DECISION AND SUPPORT SYSTEM (WDSS) EVALUATION AND TRANSITION ISSUES (MR. WHEELER)

No further funding was found for the continued NSSL contract. A teleconference between all interested parties was held in late August and it was determined that the AMU should not continue with this task.

SUBTASK 5   I&M AND RSA SUPPORT (DR. MANOBIANCO/MR. WHEELER)

Mr. Wheeler was requested to review and comment on a PRC Inc. proposal to complete the Advanced MIDDS upgrade program. He also reviewed and commented on various PRC Inc. proposals which dealt with how to incorporate satellite ingest and display functions into the Advanced MIDDS display system.

2.3   TASK 005   MESOSCALE MODELING

SUBTASK 2   29 KM ETA MODEL EVALUATION (DR. MANOBIANCO)

In September, Dr. Manobianco and Mr. Nutter published and distributed the NASA contractor final report entitled *Evaluation of the 29-km Eta Model for Weather Support to the United States Space Program*. Copies of the report are available by writing to the cover page address or by sending electronic mail to pauln@fl.ensco.com.

SUBTASK 4   DELTA EXPLOSION ANALYSIS (MR. EVANS)

The primary goal of the Delta Explosion Analysis project, which is being funded by KSC under AMU options hours, is to analyze the plume resulting from the Delta 2 explosion on 17 January 1997 at 1628 UTC. Mr. Evans is using models and observations for the analysis with the principal models being RAMS, HYPACT, and REEDM and the principal observations being the WSR-88D radar observations. The RAMS model was run using both ERDAS and PROWESS. ERDAS contains version 3a of RAMS which is configured to run with 3 nested grids, inactive microphysics, and a fine grid spacing of 3 km. PROWESS contains version 4a of RAMS which is configured to run with 4 nested grids, active microphysics, and a fine grid spacing of 1.5 km.

The Melbourne WSR-88D data has been preliminarily analyzed and has provided information on the track of the cloud following the explosion. The radar is located approximately 37 km south of Cape Canaveral and scans a horizontal radial of 360 degrees at five vertical elevation angles ranging from 0.5 to 4.5 degrees every 10 minutes.

Radar reflectivity measurements of the resulting cloud provided good estimates of the location and dimensions of the cloud over a 4-h period after the explosion. The radar's beam width and volumetric averaging prevented precise measurements of the cloud dimension. However, preliminary analysis of the scan ending at 1636 UTC indicated the low level cloud was approximately 3-km long, 2-km wide, at least 2-km thick and was located 1 km from Launch Complex (LC) 17. The bottom of the cloud not be determined because the explosion occurred during one of the radar's scans. The upper level cloud was approximately 4-km long, 4-km wide, 1.5-km thick and was located 6 km east of LC 17. The top of this cloud was approximately 3200 m above the surface. Figure 6 shows the composite radar image ending at 1646 UTC. Figure 7 shows the cross section of the radar image at the same time. The cross section shows

how the plume is split into two distinct clouds with an upper cloud to the east and a lower cloud to the south of LC 17.

Preliminary data indicate that HYPACT simulations made using data from the PROWESS version of RAMS and data from the ERDAS version of RAMS performed similarly. HYPACT moved the lower plume to the south and slightly to the west in a direction close to the observed path. However, the location where HYPACT moved the plume onshore was approximately 15 km south of the observed location (Figs. 8 and 9).

Modeling analysis and data reduction will continue on this task and final results will be included in the final report due out in February 1998.
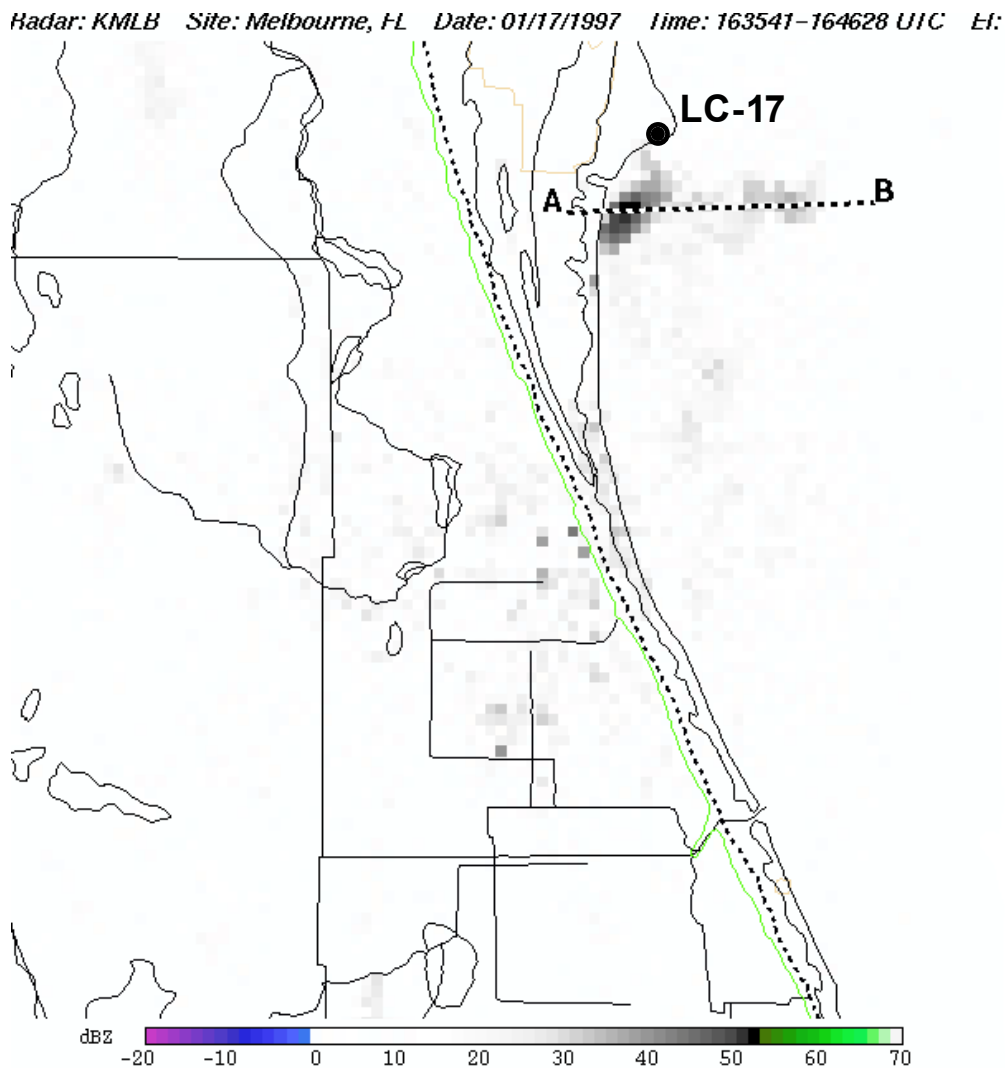
Figure 6.   Composite radar image from Melbourne WSR-88D for 10-minute scan ending at 1636 UTC. A-B line indicates cross section shown in Figure 7.

NEXRAD reflectivity cross section – Melbourne, FL
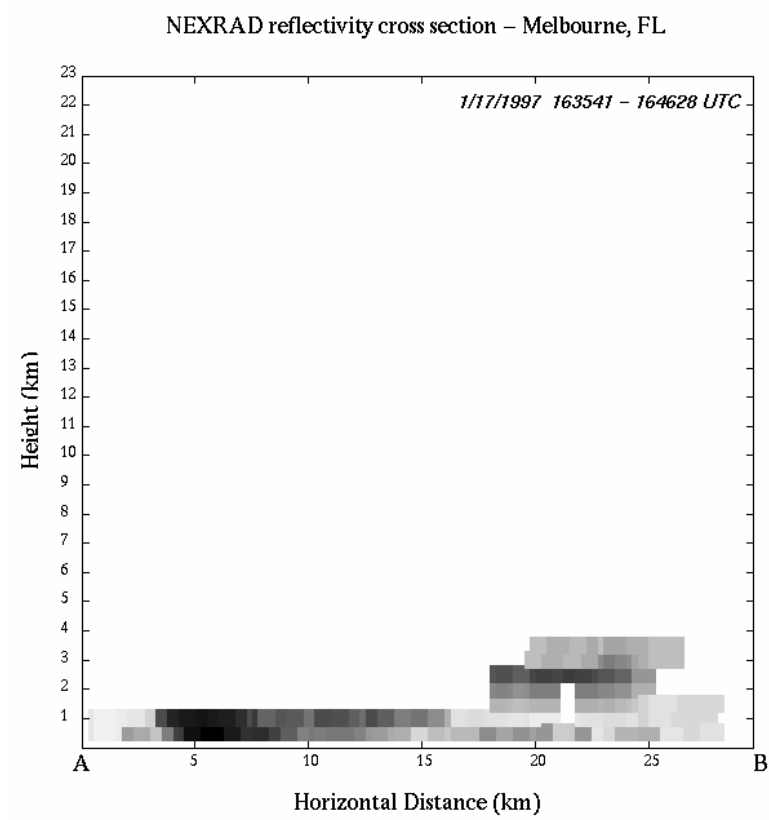
Figure 7.   Cross section of composite radar image for 1636 UTC. East-west cross section is for location shown in Figure 6.
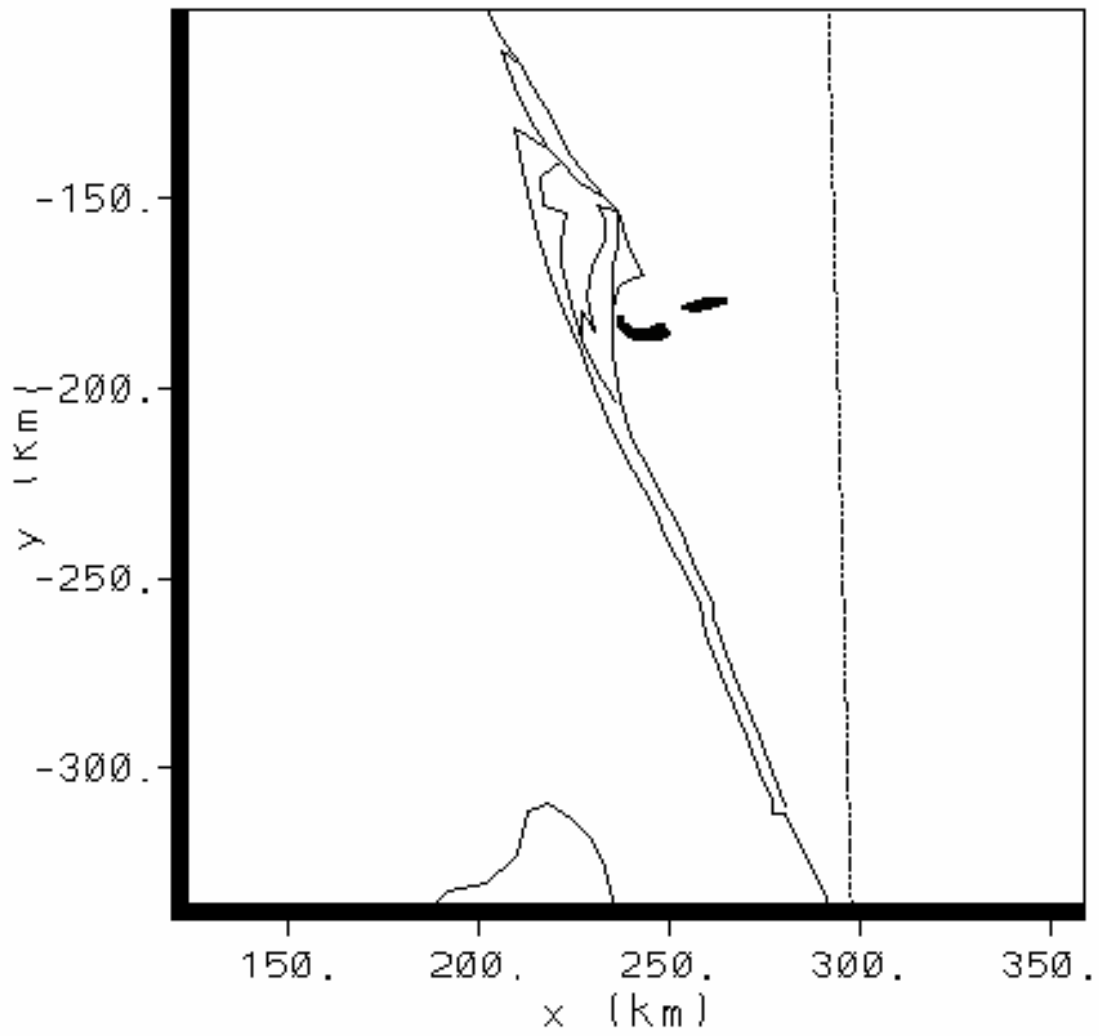
Figure 8.   HYPACT model predictions from PROWESS-RAMS showing predicted plume locations at approximately 30 minutes after explosion.
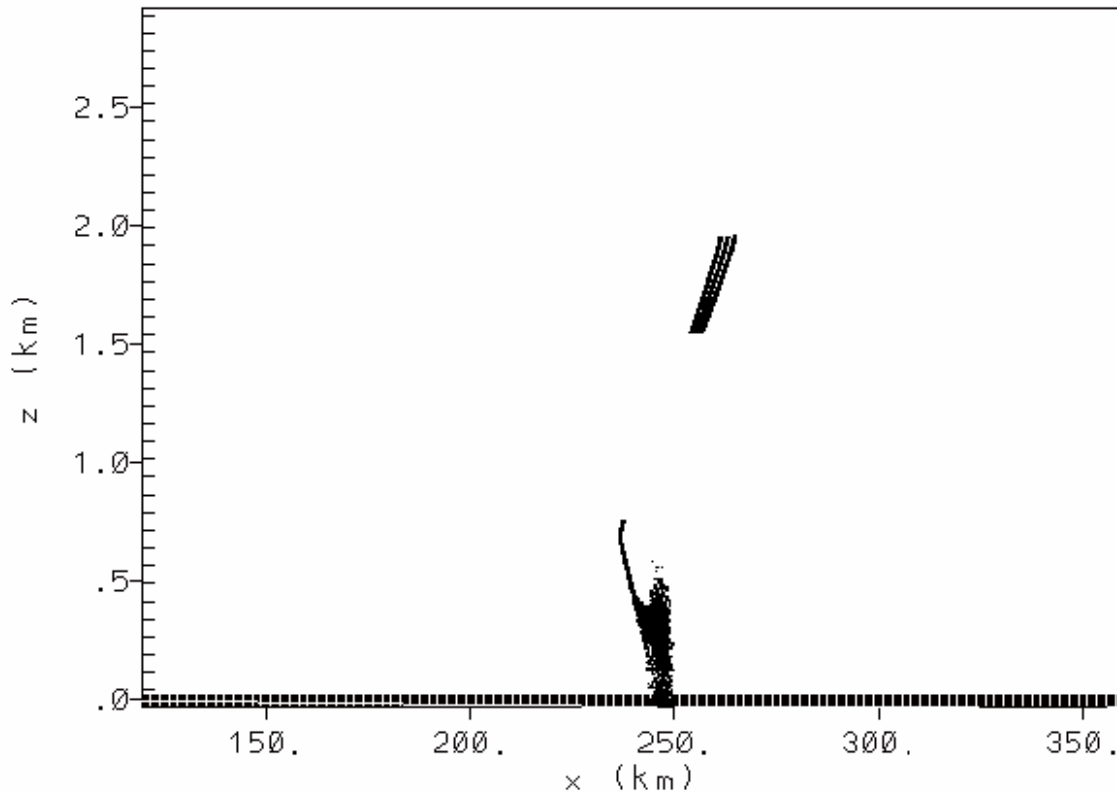
Figure 9.   HYPACT model predictions from PROWESS-RAMS showing predicted cross-section of plume locations at approximately 30 minutes after explosion.

SUBTASK 5   MODEL VALIDATION PROGRAM (MR. EVANS)

The Model Validation Program (MVP) Data Analysis project began during July. The primary purpose of this project is to produce RAMS and HYPACT data for the three MVP sessions conducted at Cape Canaveral in 1995-96. The first 2 tasks accomplished were 1) getting HYPACT running on the PROWESS workstations and 2) determining the source configuration to be used for HYPACT input. To determine the source configuration for MVP Session III, we consulted with the MVP team and made various test model simulations.

Several different HYPACT configurations were tested for the MVP Session III data to determine the best configuration with respect to the source term to represent the MVP releases. The configuration options are number of particles, source length, width and height, source duration, and grid spacing. A SAS software routine was developed to analyze and display the GPS blimp locations and was used to help determine some of the input source characteristics. We also modified HYPACT to get the output to conform to the desired format.

Once the source configuration was finalized, the RAMS-PROWESS HYPACT simulations for all of the continuous plume releases for Session III were made. Puff releases were not modeled because sample data was not collected for the releases. The data will provided to NOAA/ATDD when the

HYPACT Session III analysis is completed. RAMS and HYPACT data for Sessions I and II will be modeled and compiled in the next tasks for this project.

Figure 10 shows an example of a PROWESS HYPACT plume generated for the surface layer for MVP Release 301 on 27 April 1996. Figure 11 shows an example of the resulting surface layer concentrations from MVP Release 301 on 27 April 1996.
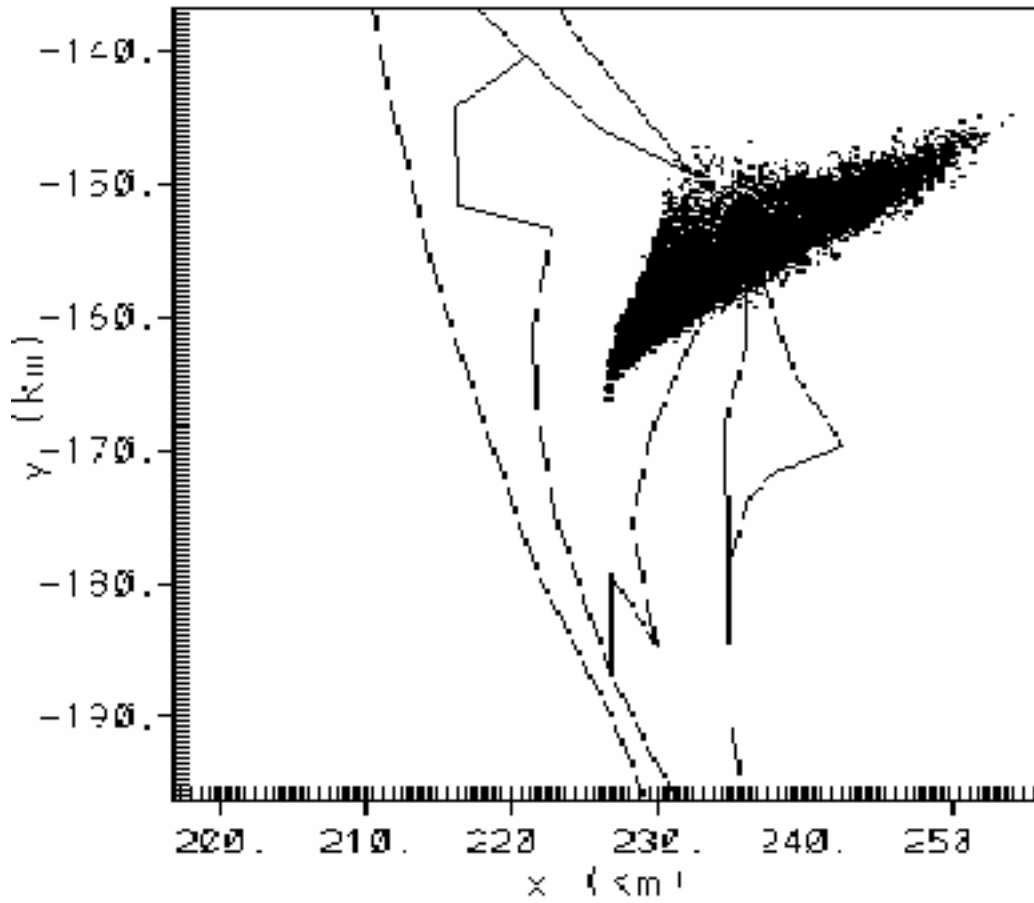
Figure 10.   An example of a PROWESS HYPACT plume generated for the surface layer for MVP Release 301 on 27 April 1996.

15

RAMS/HYPACT
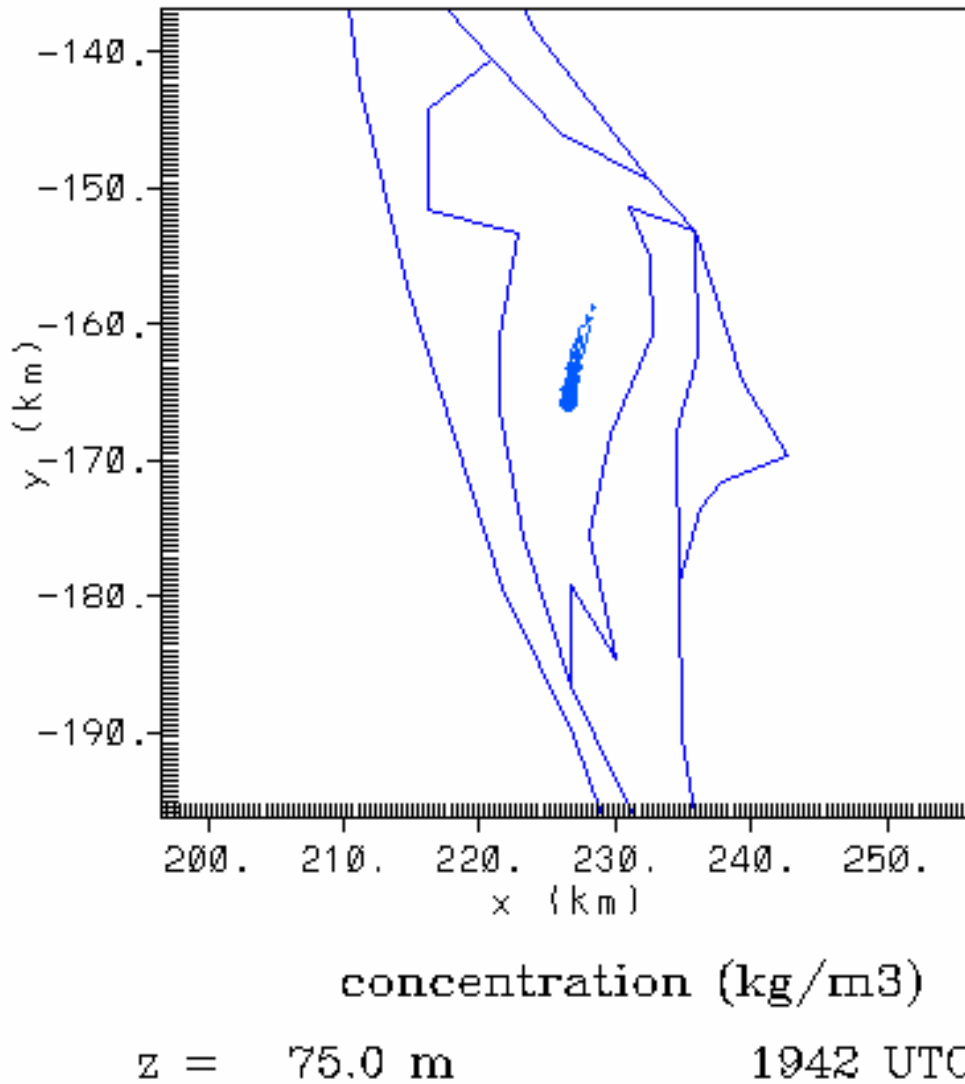
Figure 11.   An example of the resulting surface layer concentrations from MVP Release 301 on 27 April 1996.

SUBTASK 6   EXTEND 29-KM ETA MODEL OBJECTIVE EVALUATION (MR. NUTTER)

In July, Mr. Nutter, Dr. Manobianco, and Dr. Taylor established the formal task plan for the extension of the objective portion of the meso-eta model evaluation. Previously under subtask 2, the AMU conducted an evaluation of the National Center for Environmental Prediction (NCEP) 29-km eta (meso-eta) model. The purpose of the evaluation was to determine if the meso-eta model is capable of providing enhanced short range (12–24 h) forecast guidance in support of 45 WS, SMG, and NWS MLB

operational weather requirements. The evaluation protocol consisted of both objective and subjective methodologies and focused on a warm season period from May through August 1996 and a cool season period from October 1996 through January 1997 (Nutter and Manobianco 1997, Manobianco and Nutter 1997).

As part of ongoing efforts to improve the accuracy and utility of forecast products, NCEP is continuing to update the configuration, initialization, and physical parameterizations of the eta model. These updates could modify some of the seasonal error characteristics identified by the AMU's objective verification of surface and upper air forecasts at selected locations. Moreover, conclusions drawn about errors from the objective verification are based on limited samples of forecasts and observations collected during each single-season evaluation period. For these reasons, the objective component of the meso-eta evaluation is extended to include a second warm and cool season period from May through August 1997 and October 1997 through January 1998, respectively. A comparison between results from the 1996 and 1997 seasons will highlight changes in the error characteristics which may occur at selected locations in response to updates in the meso-eta model configuration. The comparison is also useful for model users since the 1997-98 results will be more representative of the meso-eta model's current capabilities.

In August, Mr. Nutter began to modify existing software and develop new software necessary to perform statistical verification of meso-eta model point forecasts. In September, Dr. Manobianco processed weather observations collected during the extended warm season from 1 May through 31 August 1997. Meanwhile, Mr. Nutter began the analysis of surface forecasts and observations collected during the 1996 and 1997 warm season periods. In the following sections, some preliminary results of this work are presented.

Eta Model Overview

In August 1995, NCEP implemented an operational mesoscale version of the eta model with a horizontal grid point resolution of 29 km and 50 vertical layers (Mesinger 1996). The most recent change to the eta model occurred on 18 February 1997 when components of the radiation, cloud, and surface moisture processes were updated. NCEP has since developed a two-stage plan to create a mesoscale version of the eta model which runs four times per day (0000, 0600, 1200 and 1800 UTC). During stage one, NCEP will upgrade the 48-km "early" eta model configuration by increasing the horizontal grid point resolution to 32 km with 45 vertical levels. Subsequently in stage two, NCEP will advance the current 29-km eta model run time to 0600 and 1800 UTC and make the grid point resolution consistent at 32 km with 45 vertical levels. As of early September 1997, the two-stage plan had not yet been implemented but is expected during fall 1997. General information regarding these changes is provided on the internet by a list of frequently asked questions (FAQ) at the NCEP Environmental Modeling Center (EMC; http://nic.fb4.noaa.gov:8000/research/FAQ-eta.html). Additional details about the numerics and physics of the eta model are provided by Black (1994), Rodgers et al. (1996), and Zhao et al. (1997).

Data

Local station or point forecasts from the 0300 UTC and 1500 UTC meso-eta model cycles are obtained from NOAA's Information Center (NIC) FTP server. The station forecasts are extracted from the meso-eta model grid point nearest to selected rawinsonde observation sites. Under the current configuration, meso-eta point forecasts provide hourly data for a duration of 33 h.

For comparison, hourly surface observations are collected from the Shuttle Landing Facility, FL (TTS), Edwards Air Force Base, CA (EDW), and Tampa, FL (TPA). In addition, rawinsonde observations are collected twice daily from EDW, Cape Canaveral Air Force Station, FL (XMR), and Tampa Bay, FL (TBW). Although surface and rawinsonde observations are not collocated at XMR and TBW, the available sites differ by not more than about 30 km (i.e. the meso-eta model grid spacing). In order to

avoid confusion, all subsequent references to rawinsonde and surface verification will use the rawinsonde station identifiers (XMR, TBW, EDW).

The AMU began collection of forecast and observed data at these locations in May 1996. For this evaluation, a warm season period is defined over the months May through August while a cool season period extends from October through January. At the end of January 1998, two sets of forecast and observed data for both the warm and cool seasons will be available for evaluation of meso-eta forecast accuracy.

Analysis

The objective verification of the meso-eta model focuses on the overall accuracy of wind, temperature, and moisture forecasts at the three stations mentioned above. The statistical measures used to quantify model forecast errors are the bias (forecast – observed), root mean square (RMS) error, and error standard deviation. Using these statistics, point forecasts from the meso-eta model are verified against standard surface and upper air observations. For quality control, gross errors in the data are screened manually and corrected, if possible. Error values which are greater than three standard deviations from the mean forecast minus observed differences are excluded from the final statistics. This procedure is effective at flagging bad data points and removes less than one percent of the data. A more extensive discussion of the evaluation criteria is presented by Nutter and Manobianco (1997) and Manobianco and Nutter (1997).

While examining overall forecast accuracy for a given parameter, it is desirable to determine the statistical significance of differences between 1996 and 1997 seasonal means. It is assumed the distribution of differences in sample means between subsequent seasons is approximately normal. This assumption follows from the Central Limit Theorem and improves with larger samples (Walpole and Meyers 1989) such as those created by considering averages over the entire 33-h forecast period. In order to assess the significance of differences between 1996 and 1997 sample means, the standardized z-statistic is calculated for each parameter and compared with the normal distribution. A two-tailed comparison using a 99% confidence level (α = 0.01) has critical z-values of ±2.58. Differences in seasonal mean forecasts, observations, or forecast errors for a given parameter are not statistically significant if the corresponding z-statistic lies within this range (Walpole and Meyers 1989).

Results

The results presented in this section focus on the objective verification of 2-m temperature and 10-m wind speed as function of forecast duration for the twin warm season periods at XMR, TBW, and EDW. In particular, results from the 1996 evaluation are compared with those obtained in 1997. Verification of forecasts for upper air and other surface parameters is not discussed at this time.

2-m Temperature

At XMR and TBW, 2-m temperature biases range from about 1 to -3 ˚C during both the 1996 and 1997 warm seasons (Figs. 12a, b). The mean errors tend to follow a diurnal cycle that is most pronounced at EDW during the 1996 warm season (Fig. 12a). In 1997 however, the diurnal cycle is not as evident throughout the forecast period as 2-m temperature forecasts for EDW are on average 2 to 6 ˚C colder than observed (Fig. 12b).

The bias and standard deviation represent systematic and non-systematic model errors which both make contributions to the total RMS error. In conjunction with larger negative biases at EDW, RMS errors reach nearly 6 ˚C and are correspondingly larger than RMS errors at XMR and TBW during both warm season periods (Figs. 12c, d). On the other hand, error standard deviations at EDW are generally comparable in magnitude to those at XMR and TBW (Figs. 12e, f). Therefore, the larger contribution to

the total error at EDW is from the bias or systematic model error. One possible explanation for this systematic model deficiency in 2-m temperature forecasts at EDW may be that forecast point data extracted from the model are almost 250 m lower than the actual station elevation.
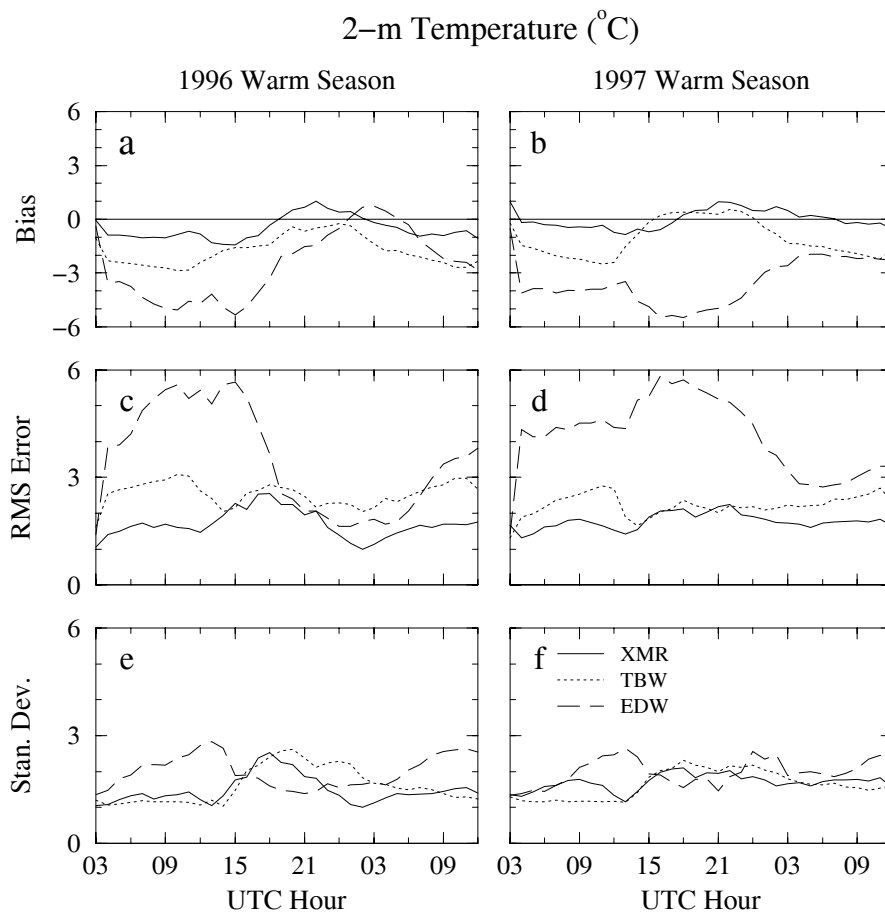
2–m Temperature (^{o}C)

Figure 12.   Bias, RMS error, and error standard deviation of 2-m temperature (°C) for XMR (solid lines), TBW (dotted lines), and EDW (long dashed lines). Panels a, c and e (b, d and f) show May through August 1996 (1997) error statistics plotted as a function of verification time.

At all three stations, differences between 1996 and 1997 seasonally-averaged model errors in 2-m temperature are statistically significant at the 99% confidence level (Table 2, bottom row). Further investigation reveals that while seasonal differences in average forecast temperatures are statistically significant, the corresponding differences in observed means are not (Table 2). These results suggest that the eta model update package implemented 18 February 1997 may have affected warm season forecast accuracy for 2-m temperatures at these locations.

The updates to the eta model's radiation package were designed to reduce the net shortwave radiation at the ground and thereby help control excessive daytime heating (NCEP-EMC internet FAQ, 1997). Indeed, comparison of Figs. 12a, b reveals that the strong diurnal bias cycle at EDW during the 1996 warm season is flattened and becomes a more constant negative value in 1997. Apparently, the February 1997 model updates subsequently helped reduce daytime temperatures at EDW. The increased negative bias in forecast temperatures extends into the nighttime hours as well. In fact, an hourly calculation of the standard *z*-statistic for EDW (not shown) indicates that between 1996 and 1997, a

statistically significant decrease in mean warm season temperature forecasts occurs at every hour between 1700 and 0500 UTC (Figs. 12a, b).

Although statistical results suggest that the model update package may have affected 2-m temperature forecast accuracy, sensitivity tests are required in order to formally validate this speculation and to determine exactly why the forecasts are affected. As an example, seasonal changes in mean forecast temperatures at XMR and TBW (not shown) are statistically significant but are on average warmer in 1997 than 1996.

Table 2. Standardized *z*-statistics for 1996 - 1997 differences in 33-h mean warm season 2-m temperature forecasts, observations, and forecast errors. For a two-tailed comparison with the normal distribution, shaded values are not statistically significant at the 99% (α = 0.01) confidence level.

	XMR	TBW	EDW
Forecast	-7.33	-6.48	7.59
Observed	-1.12	1.63	2.47
Model Error	-10.48	-13.66	14.63

10-m Wind Speed

Warm season biases in 10-m wind speed forecasts range from 0 to -2 m s^{-1} at EDW and from -1 to 2 m s^{-1} at XMR and TBW (Figs. 13a, b). In general, 10-m wind speed forecasts at XMR and TBW are quite good on average while those at EDW are slightly slower than observed. Since biases are small and error standard deviations are comparable in magnitude to the RMS error, much of the total error in the forecasts is derived from the non-systematic or random error component in either the forecasts or observations.

At XMR, seasonal differences in the average forecast 10-m wind speed are not statistically significant at the 99% confidence level (Table 3). However, corresponding differences in seasonal mean wind speed forecast errors and observations are significant at XMR (Table 3). Together, these results suggest that seasonal changes in mean 10-m wind speed due to interannual variability may be larger at XMR than changes due to the given model updates. On the other hand, changes in mean winds speeds between 1996 and 1997 at TBW are not statistically significant for observations, forecasts, and forecast errors (Table 3). Finally, corresponding differences at EDW are statistically significant for both forecasts and observations, but not for the forecast errors. The lack of uniformity to the significance of seasonal changes in mean wind speed at XMR, TBW, and EDW is not surprising since the eta model updates implemented in February 1997 were not explicitly designed to affect wind speed forecasts.

Table 3. As in Table 2, except *z*-statistics for 10-m wind speed are presented.

	XMR	TBW	EDW
Forecast	-2.22	0.39	17.40
Observed	-6.01	2.35	4.88
Model Error	3.77	-0.88	1.01

Summary

Preliminary results of the AMU's twin-season objective verification of the 29-km eta model have been highlighted in the previous sections. The evaluation is designed to measure the accuracy of local meso-eta point forecasts in support of operational forecast requirements for 45 WS, SMG, and NWS MLB. By extending the evaluation across two warm and cool season periods, the effects of model changes on forecast accuracy at XMR, TBW, and EDW can be investigated.

Preliminary results presented in this section suggest that the bundle of eta model updates implemented 18 February 1997 may have affected the accuracy of warm season 2-m temperature forecasts at XMR, TBW, and EDW. Examination of seasonal changes in 10-m wind speed forecasts at these stations is inconclusive. When complete, the project will include analysis of several surface and upper air parameters. The final analysis will include stratification by model run time and different wind regime classifications.
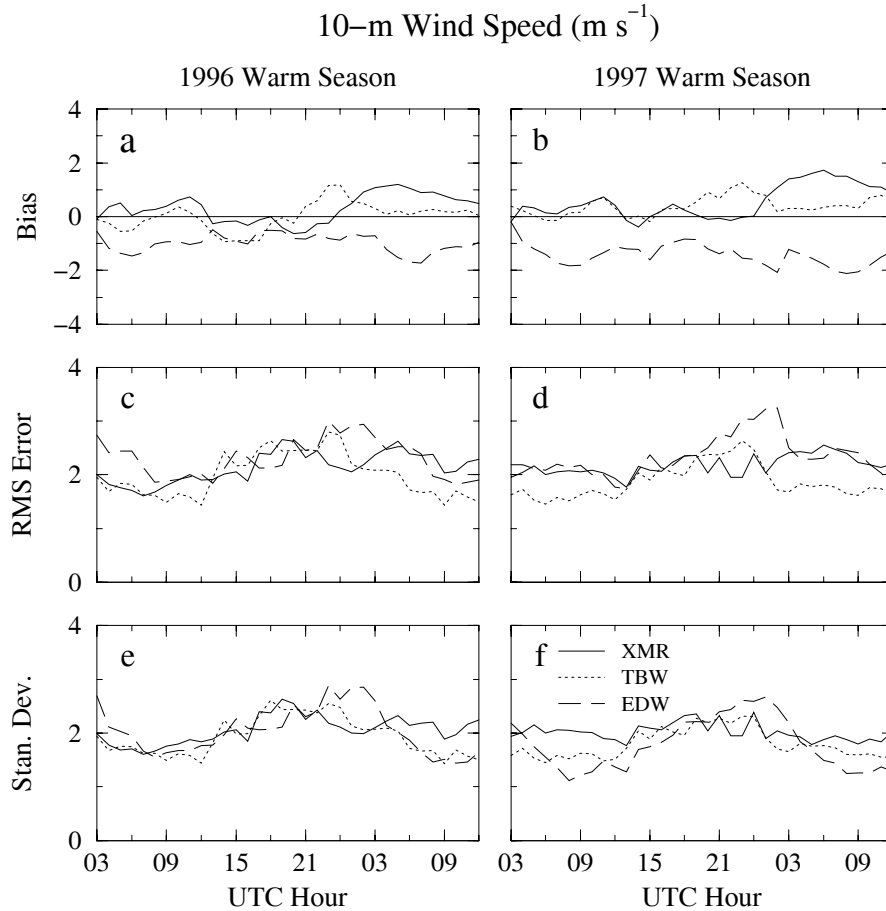
Figure 13.   Bias, RMS error, and error standard deviation of 10-m wind speed (m s-1) for XMR (solid lines), TBW (dotted lines), and EDW (long dashed lines). Panels a, c and e (b, d and f) show May through August 1996 (1997) error statistics plotted as a function of verification time.

References

Black, T. L., 1994: The new NMC mesoscale eta model: description and forecast examples. *Wea. Forecasting*, 9, 265-278.

Manobianco, J. M., and P. A. Nutter, 1997: Evaluation of the 29-km Eta Model for Weather Support to the United States Space Program. NASA Contractor Report CR-205409, Kennedy Space Center, FL, 103 pp. [Available from ENSCO, Inc., Applied Meteorology Unit, 445 Pineda Ct., Melbourne, FL 32940, USA]

Mesinger, F., 1996: Improvements in quantitative precipitation forecasts with the eta regional model at the National Centers for Environmental Prediction: The 48-km upgrade. *Bull. Amer. Meteor. Soc.*, 11, 2637-2649.

Nutter, P. A., and J. M. Manobianco, 1997: Evaluating the potential utility of the meso-eta model for weather support to the US space program. Preprints, *7th Conference on Aviation, Range and Aerospace Meteorology*, Long Beach, CA, Amer. Meteor. Soc., 420-425.

Rodgers, E., T. L. Black, D. G. Deaven, G. J. DiMego, Q. Zhao, M. Baldwin, N. Junker, and Y. Lin, 1996: Changes to the operational "early" eta analysis/forecast system at the National Centers for Environmental Prediction. *Wea. Forecasting*, 11, 391-413.

Walpole, R. E., and R. H. Meyers, 1989: Probability and Statistics for Engineers and Scientists. Macmillan, Inc., New York, 765 pp.

Zhao, Q., T. L. Black and M. E. Baldwin, 1997: Implementation of the cloud prediction scheme in the Eta model at NCEP. *Wea. Forecasting*, 12, 697-712.

SUBTASK 7   DATA ASSIMILATION MODEL / CENTRAL FLORIDA DATA DEFICIENCY (DR. MANOBIANCO)

In July, Dr. Manobianco, Mr. Nutter, and Dr. Taylor established the formal plan for the data assimilation model / central Florida data deficiency task. This task has three main components.

- Identify all existing meteorological data sources (government, agricultural, utility, etc.) that lie within 160 km of KSC/CCAS,

- Identify an appropriate data assimilation model that incorporates and analyses all existing central Florida meteorological data sources in a dynamically consistent manner, and

- Implement a working prototype of the data integration model and perform a proof-of-concept test through post-analysis of selected weather events for two days.

The ultimate goal for running a local data integration system (LDIS) is to generate products which may enhance weather nowcasts and short-range (< 6 h) forecasts issued in support of 45 WS, SMG, NWS MLB operational weather requirements. A LDIS has the potential to provide added value because it incorporates data which are available only in central Florida and is run at finer spatial and temporal resolutions over smaller domains than current national-scale, operational models (such as the Rapid Update Cycle; RUC).

The LDIS combines all available data in a dynamically consistent manner and produces gridded analyses of primary variables such as temperature, wind, etc. and diagnostic quantities such as vorticity, divergence, etc. at specified temporal and spatial resolutions. In this regard, the LDIS along with suitable

visualization tools may provide users with a more complete and comprehensive understanding of evolving weather than could be developed by individually examining the disparate data sets over the same area and time. Initially, the LDIS will not run in real-time; however, its potential added value to nowcasting/short range forecasting will be assessed by performing analyses on two selected days. The following sections highlight AMU progress on the task during the past quarter.

Data Integration System

There are currently two assimilation systems being considered as candidates for the LDIS. These include the Local Analysis and Prediction System (LAPS; McGinley 1995) and the ARPS (Advanced Regional Prediction System) Data Assimilation System (ADAS; Brewster 1996). LAPS is available from NOAA's Forecast Systems Laboratory (FSL; Boulder, CO) and ADAS/ARPS is available from the Center for Analysis and Prediction of Storms (CAPS) at the University of Oklahoma (Norman, OK). LAPS and ADAS can be configured to run at different horizontal/vertical resolutions over any geographic domain. In fact, both systems have been used to generate meso-beta scale analyses by assimilating a multitude of data including aircraft, radar, profiler, satellite, surface, and rawinsonde observations (Stamus and McGinley 1996; Droegemeier et al. 1996).

Initial Configuration

When configured for local use, it is anticipated that the LDIS will be run over an outer grid (inner) grid with a horizontal resolution on the order of 10 (2) km and at least 40 unevenly spaced vertical levels. The horizontal extent and distribution of grid points for the 10- and 2-km grids are shown in Figs. 14 and 15, respectively. The 10-km (2-km) analysis domain covers 400 x 400 km (160 x 160 km). The RUC will be used as background field for 1-h analyses of all observational data on the 10-km domain. Currently, the RUC assimilates observations every 3 h at a horizontal grid point resolution of 60 km with 25 vertical levels. NCEP is currently testing a 40-km, 40-level version of the RUC which assimilates observations every 1 h (Kalnay et al. 1996). The resulting 10-km products will then be used as background fields for analyses on the 2-km domain. This nested-grid configuration and cascade-of-scales analysis follows that used for the terminal winds analysis in the Integrated Terminal Weather System (ITWS; Cole and Wilson 1995). With such an approach, it is possible to analyze for different temporal and spatial scales of weather phenomenon measured by various sensors (see next section).
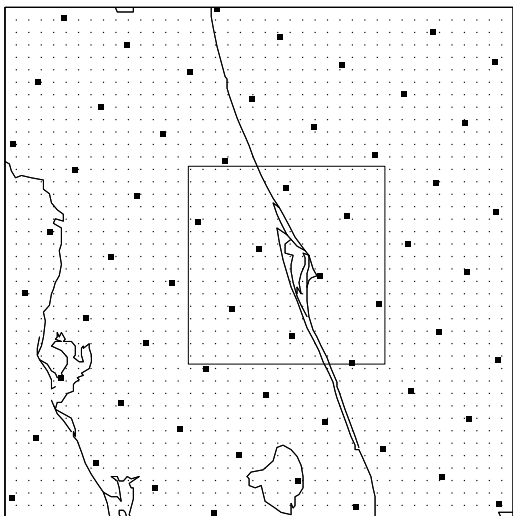
Figure 14. Proposed domain for the 10-km analysis grid. Grid point locations are given by dots. Squares denote 60-km RUC grid point locations. The outline of the 2-km domain is shown by the inner square.
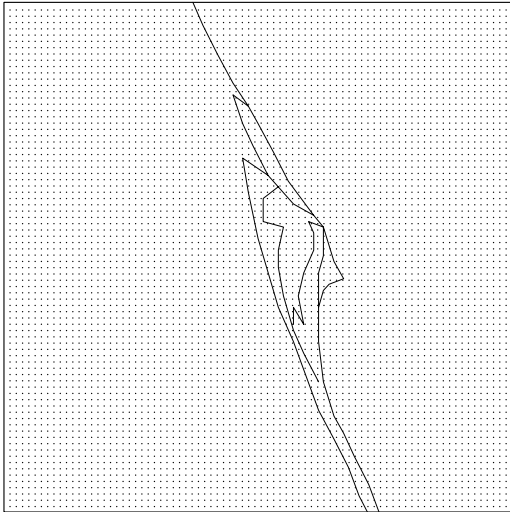
Figure 15. Proposed domain for the 2-km analysis grid. Grid point locations are given by dots.

Data Coverage / Resolution

The utility of a LDIS depends to a large extent on the reliability and availability of both in-situ and remotely-sensed observational data. All existing observational data within 160 km of KSC/CCAS which can be incorporated by a LDIS are listed in Table 4. A representative distribution of the observational data listed in Table 4 is depicted in Fig. 16. The station or observation locations were obtained by collecting sample data sets on different days and times. Actual data values are not shown because Fig. 16 is designed only to illustrate approximate data coverage and resolution. The data availability, coverage, and density for each case study will likely depend on the days selected. Note that samples of visible satellite, aircraft/pilot and WSR-88D data coverage are not shown in Fig. 16.

Table 4. Summary of available data including source, variable, frequency and reference (if appropriate).

Data Type	Data Source	Variable	Frequency (min)	Reference
GOES-8 Satellite				
VIS/IR imagery	CCAS MIDDS	brightness T	15	Menzel and Purdom (1994)
Soundings	NESDIS ORA/FPDT	T, q	60	Gray et al. (1996)
Cloud drift winds	NESDIS ORA/FPDT	u, v	360	Neiman et al. (1997)
Water vapor winds	NESDIS ORA/FPDT	u, v	360	Veldon et al. (1997)
Surface				
METAR	CCAS MIDDS	u, v, T, T_d, p	60	----
Buoy/ship	CCAS MIDDS	u, v, T, T_d, p, SST	60	----
KSC/CCAS towers	CCAS MIDDS	u, v, T, RH	5	----
Central Florida mesonet	NWS Tampa, FL	u, v, T, T_d, p	60	http://www.marine.usf.edu
Upper Air				
Rawinsonde	CCAS MIDDS	u, v, T, RH	720	----
Radar				
WSR-88D	NWS Melbourne, FL (Level II archive)	radial wind, reflectivity	6	----
Aircraft				
Aircraft/pilot reports	CCAS MIDDS	u, v, T, ICE, TURB, cloud	Variable	----
ACARS	NOAA FSL	u, v, T	7.5	Benjamin et al. (1991)
KSC/CCAS Profiler				
915 MHz / RASS	AMU	u, v, T_v	15	----
50 MHz	CCAS MIDDS	u, v	5	----

VIS = visible; IR = infrared; NESDIS = National Environmental Satellite Data and Information Service

ORA = Office of Research Applications; FPDT = Forecast Products Development Team

MIDDS = Meteorological Interactive Data Display System

u = east-west wind; v = north-south wind; T = temperature; T_d = dew point T; T_v = virtual T; SST = sea-surface T

RH = relative humidity; q = specific humidity; p = pressure; ICE = icing; TURB = turbulence

ACARS = Aeronautical Radio, Inc. (ARINC) Communications, Addressing and Reporting System

RASS = Radio Acoustic Sounding System
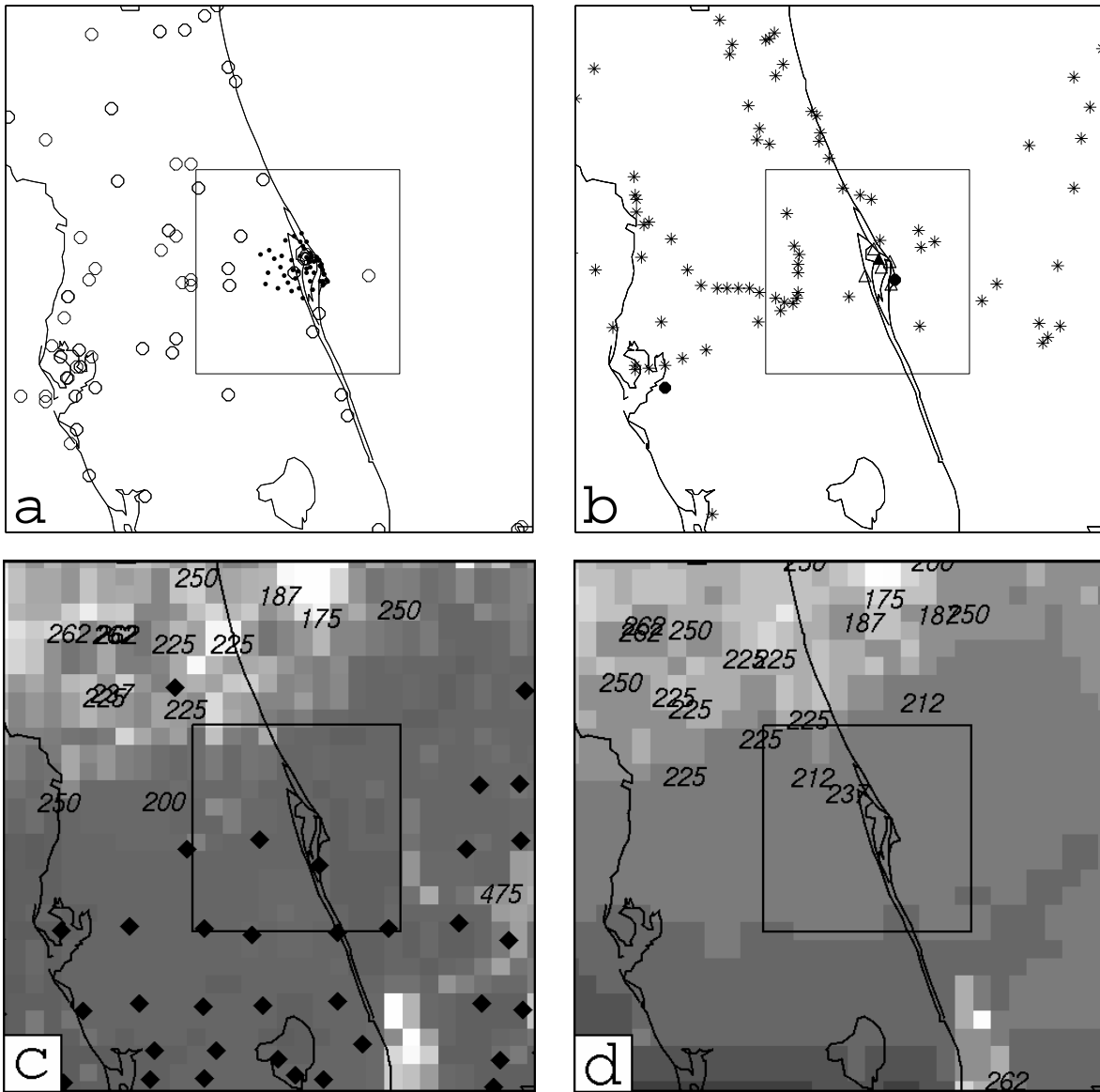
Figure 16.   Sample distribution of selected observations listed in Table 4 with the 10-km and 2-km analysis domains shown in Fig. 14.   Panel (a) shows METAR, buoy/ship and central Florida mesonet stations (octagons) and KSC/CCAS towers (filled circles).   Panel (b) shows location of sample ACARS data (asterisks), rawinsondes (solid octagons), 915 MHz profilers (open triangles), and 50 MHz profiler (solid triangle).   Panel (c) shows location of GOES-8 cloud-drift winds indicated by pressure level (mb) and GOES-8 soundings (solid diamonds) plotted over the GOES-8 IR image.   Panel (d) shows the location of GOES-8 water vapor winds also indicated by pressure level (mb) plotted over the GOES-8 water vapor image.   All satellite products are derived from GOES-8 data at 1045 UTC 25 September 1997.   GOES-8 images are shown at a horizontal resolution of ~16 km.

Data density and coverage in east central Florida varies considerably depending on level in the atmosphere and distance from KSC/CCAS. The largest variability in horizontal/vertical coverage and density occurs with aircraft data, satellite soundings, and satellite winds. The maximum density of near-

surface wind and temperature observations occurs at the center of the 2-km analysis domain with the KSC/CCAS tower network (Fig. 16a). The distribution of other surface observations from METAR, buoy/ship and Florida mesonet stations shows a concentration over the central portion of the peninsula with almost no surface data available over the western Atlantic in either the 10-km or 2-km domain (Fig. 16a). The one 50-MHz and five 915-MHz boundary layer profilers (with Radio Acoustic Sounding Systems) are located around KSC/CCAS so they provide high temporal resolution wind and virtual temperature measurements over limited areas near the center of either analysis domain (Fig. 16b). Finally, the two rawinsonde sites at Tampa, FL and Cape Canaveral, FL (Fig. 16b) provide the least spatial and temporal resolution of all sensors listed in Table 4.

Commercial aircraft observations of wind and temperature are typically concentrated at flight levels in the upper troposphere and at lower levels during aircraft ascent/descent near airports (Schwartz and Benjamin 1995). The sample ACARS data plotted in Fig. 16b cover a 1-h period centered on 2200 UTC 12 May 1997 and represent the maximum number of observations available for a given hour on this day. These data were obtained from the experimental aircraft data display at NOAA FSL (http://acweb.fsl.noaa.gov).

Vertical profiles of temperature and moisture are retrieved hourly from GOES-8 sounder data at a horizontal resolution of ~50 km (Gray et al. 1996). However, soundings are available only in cloud-free areas so horizontal coverage can vary depending on the time of day, synoptic conditions, etc. The locations of GOES-8 soundings at 1045 UTC 25 September 1997 are plotted in Fig. 16c along with the corresponding GOES-8 IR image. GOES-8 soundings are concentrated primarily in the cloud-free zone oriented southwest-northeast across the southern half of the Florida peninsula.

The vertical and horizontal distribution of cloud-drift winds depends primarily on tracking cloud features and diagnosing heights to assign the vertical level for the associated wind (Neiman et al. 1997). The coverage of water vapor winds also depends on tracer selection and height assignment although water vapor wind vector targets are selected in both cloudy and cloud-free regions (Veldon et al. 1997). The locations of GOES-8 cloud-drift winds at 1045 UTC 25 September 1997 are plotted in Fig. 16c. A similar distribution of GOES-8 water vapor winds at the same time is shown in Fig. 16d along with the corresponding GOES-8 water vapor image. The vertical distribution of cloud-drift and water vapor winds is indicated by the pressure level plotted at the observation location (Figs. 16c and 16d). The heights of the cloud drift (water vapor) winds over the 10-km domain at 1045 UTC 25 September range from 475 to 175 mb (262 to 175 mb). In contrast to GOES-8 soundings, cloud-drift and water vapor winds are found where clouds and moisture features can be can be identified by the tracer selection and tracking algorithms (Neiman et al. 1997; Veldon et al. 1997).

Ongoing/Future Work

It is important to reiterate that the prototype LDIS will not initially be configured to run in real-time. The AMU will complete the installation/testing of the LDIS, develop software to reformat those data sets in Table 4 which are not currently ingested by the LDIS, select two case study days, collect/acquire all available data, and then run the analyses for each day. One day will be chosen with numerous interactions of mesoscale weather features across central Florida while an alternate day will be chosen when there is relatively little weather present. The case studies will be designed to highlight the capabilities and limitations of the LDIS and evaluate the impact of non-incorporation of specific data sources on the utility of the subsequent analyses.

References

Benjamin, S., K. A. Brewster, R. Brummer, B. J. Jewett, T. W. Schlatter, T. L. Smith, and P. A. Stamus, 1991: An isentropic three-hourly data assimilation system using ACARS aircraft observations. *Mon. Wea. Rev.*, **119**, 888-906.

Brewster, K., 1996: Application of a Bratseth analysis scheme including Doppler radar data. Preprints, *15th Conf. on Weather Analysis and Forecasting*, Norfolk, VA, Amer. Meteor. Soc., 92-95.

Cole, R. E., and W. W. Wilson, 1995: ITWS gridded winds product. Preprints, *6th Conf. on Aviation Weather Systems*, Dallas, TX, Amer. Meteor. Soc., 384-388.

Droegemeier, K. K., and Co-authors, 1996: The 1996 CAPS spring operational forecasting period: real-time storm-scale NWP, Part I: Goals and methodology. Preprints, *11th Conf. on Numerical Weather Prediction*, Norfolk, VA, Amer. Meteor. Soc., 294-296.

Gray, D. G., C. M. Hayden, and W. P. Menzel, 1996: Review of quantitative satellite products derived from GOES-8/9 imagery and sounder instrument data. Preprints, *8th Conf. on Satellite Meteor. and Oceano.*, Atlanta, GA, Amer. Meteor. Soc., 159-163.

Kalnay, E., G. DiMego, S. Lord, H-L. Pan, M. Iredell, M. Ji, D. B. Rao, and R. Reynolds, 1996: Recent advances in modeling at the National Centers for Environmental Prediction. Preprints, *11th Conference on Numerical Weather Prediction*, Norfolk, VA, Amer. Meteor. Soc., J3-J8.

McGinley, J. A., 1995: Opportunities for high resolution data analysis, prediction, and product dissemination within the local weather office. Preprints, *14th Conf. on Weather Analysis and Forecasting*, Dallas, TX, Amer. Meteor. Soc., 478-485.

Menzel, P. W., and J. F. W. Purdom, 1994: Introducing GOES I: The first of a new generation of geostationary operational environmental satellites. *Bull. Amer. Meteor. Soc.*, **75**, 757-781.

Neiman, S. J., W. P. Menzel, C. M. Hayden, D. Gray, S. T. Wanzong, C. S. Veldon, and J. Daniels, 1997: Fully automated cloud-drift winds in NESDIS operations. *Bull. Amer. Meteor. Soc.*, **78**, 1121-1133.

Schwartz, B., and S. G. Benjamin, 1995: A comparison of temperature and wind measurements from ACARS-equipped aircraft and rawinsondes. *Wea. Forecasting*, **10**, 528-544.

Stamus, P. A., and J. A. McGinley, 1997: The Local Analysis and Prediction System (LAPS): Providing weather support to the 1996 summer Olympic games. Preprints, *13th Conf. on Interactive Information Processing Systems*, Long Beach, CA, Amer. Meteor. Soc., 11-30.

Veldon, C. S., C. M. Hayden, S. J. Nieman, W. P. Menzel, S. Wanzong, and J. S. Goerss, 1997: Upper-tropospheric winds derived from geostationary satellite water vapor observations. *Bull. Amer. Meteor. Soc.*, **78**, 173-195.

2.4   AMU CHIEF'S TECHNICAL ACTIVITIES (DR. MERCERET)

Dr. Merceret briefed Chris Lessman (JSC), Shuttle landing winds coordinator, on the mid-tropospheric wind change climatology and it's consequences for risk analysis. He held similar discussions with Steve Pearson and Richard Leach from MSFC.

He was asked to compile and edit the range systems section of an article on wind profilers being written by Don Beran and Tim Wilfong for the *Bulletin of the American Meteorological Society.* He assembled a team of Eastern Range, Western Range, and WSSH personnel and prepared the section as requested.

Dr. Merceret completed a revision of the NASA Public Affairs pamphlet on lightning. His paper "Risk Assessment Consequences of the Lognormal Distribution of Midtropospheric Wind Changes" was accepted by the *Journal of Spacecraft and Rockets.*

Dr. Merceret is advising John Lane, a Ph.D. candidate at the University of Central Florida, on a study of raindrop size distributions and their effect Z-R relations. The work is directed at improving the use of WSR-88D and raingauge data as ground truth for NASA's TRMM project, and will serve as Mr. Lane's doctoral dissertation. It should also prove useful in using gauges to adjust or verify radar-derived rain rates, and may lead to improved NEXRAD rain rate algorithms.

NOTICE

Mention of a copyrighted, trademarked, or proprietary product, service, or document does not constitute endorsement thereof by the author, ENSCO, Inc., the AMU, the National Aeronautics and Space Administration, or the United States Government. Any such mention is solely for the purpose of fully informing the reader of the resources used to conduct the work reported herein.

Acronyms

45 MXS	45th Maintenance Squadron
45 SW	45th Space Wing
45 WS	45th Weather Squadron
AGL	Above Ground Level
AFB	Air Force Base
AMU	Applied Meteorology Unit
CAPE	Convective Available Potential Energy
CCAS	Cape Canaveral Air Station
COMET	Cooperative program for Operational Meteorology, Education and Training
CSR	Computer Science Raytheon
DRWP	Doppler Radar Wind Profiler
EDW	Edwards Air Force Base Rawinsonde Station Identification
ERDAS	Emergency Response Dose Assessment System
FAR	False Alarm Rate
FY	Fiscal Year
GEMPAK	General Meteorological Package
GVAR	GOES Variable
HYPACT	Hybrid Particle And Concentration Transport
I&M	Improvement and Modernization
JAM	*Journal of Applied Meteorology*
JSC	Johnson Space Center
KINX	K Index
KSC	Kennedy Space Center
LDAR	Lightning Detection And Ranging
LDIS	Local Data Integration System
LIFT	Lifted Index
MDPI	Microburst Day Potential Index
MSFC	Marshall Space Flight Center
NASA	National Aeronautics and Space Administration
NCAR	National Center for Atmospheric Research
NCEP	National Center for Environment Prediction
NWS MLB	National Weather Service Melbourne
MSLP	Mean Sea Level Pressure
PAFB	Patrick Air Force Base
PROWESS	Parallelized RAMS Operational Weather Simulation System
PIREP	Pilot Report
POD	Probability Of Detection
PWAT	Precipitable Water
QC	Quality Control
RAMS	Regional Atmospheric Modeling System
REEDM	Rocket Exhaust Effluent Diffusion Model

RMS	Root Mean Square
ROCC	Range Operations Control Center
RSA	Range Standardization and Automation
RUC	Rapid Update Cycle
RWO	Range Weather Operations
SMG	Spaceflight Meteorology Group
USAF	United States Air Force
TBW	Tampa Bay area Rawinsonde Station Identification
TIM	Technical Interchange Meeting
WATADS	WSR-88D Algorithm Testing And Display System
WSR-88D	Weather Surveillance Radar - 88 Doppler
WDSS	Warning Decision Support System
XMR	Cape Canaveral Rawinsonde Station Identification

Appendix A

AMU Project Schedule 1 October 1997				
AMU Projects	Milestones	Target Begin Date	Target Completion Date	Notes/Status
MDPI	Collect/Analyze Jun-Sep 96 Data	Jul 97	Oct 97	Completed
	Compute Skill Scores	Oct 97	Nov 97	On schedule
	Documentation/ Recommendations	Nov 97	Dec 97	On schedule
Cell Trend Comparison of WATADS vs. WSR-88D	Evaluate Effectiveness/Utility of 88D Cell Trends	Apr 97	Sep 97	Completed
	Final Report	Oct 97	Nov 97	On schedule
Boundary Layer Profilers	Task Work Plan	Apr 97	Jun 97	Completed
	Data Collection	May 97	Aug 97	Completed
	Data Quality Objective	May 97	Nov 97	2-week delay
	Final Report	Nov 97	Jan 98	2-week delay
AF I&M and RSA Support	Review Document / Products, Attend Meetings / Reviews, Document Advice, Suggestions, and Comments	Jul 96	Ongoing	On schedule
Evaluate 29-km Eta Model	Final Report	Apr 97	Jun 97	Completed
Data Integration Model / Data Deficiency	Identify Mesoscale Data Sources in central Florida	May 97	May 98	On schedule
	Identify / Install Prototype Analysis System	Aug 97	Nov 97	On schedule
	Case Studies Including Data Non-incorporation	Nov 97	Apr 98	On schedule
	Final Report	May 98	Jul 98	On schedule
29-km Eta Model Evaluation Extension	Archive data for 1997/1998	May 97	Jan 98	On schedule
	Perform Analysis	Sep 97	Feb 98	On schedule
	Final Report	Mar 98	Apr 98	On schedule

AMU Project Schedule 1 October 1997				
AMU Projects	Milestones	Target Begin Date	Target Completion Date	Notes/Status
Delta Explosion Analysis	Analyze Radar Imagery	June 97	Nov 97	On Schedule
	Run Models/ Analyze Results	June 97	Dec 97	On Schedule
Model Validation Program	Final Report	Dec 97	Jan 98	
	Inventory and Conduct RAMS runs for Sessions I, II, and III	July 97	Mar 98	Session III completed
	Run HYPACT for all MVP releases	Aug 97	Mar 98	Session III PROWESS completed
	Deliver data to NOAA/ATDD	Oct 97	Mar 98	On Schedule
	Acquire met data for Titan launches	July 97	Mar 98	On Schedule
GVAR Sounder Products Evaluation	Final Report	Apr 98	Dec 98	On schedule